

International Journal of Modern Physics B  
 © World Scientific Publishing Company

## Nuclear interactions from the renormalization group

Achim Schwenk

*Department of Physics, The Ohio State University, Columbus, OH 43210 \**

We discuss how the renormalization group can be used to derive effective nuclear interactions. Starting from the model-independent low-momentum interaction  $V_{\text{low } k}$ , we successively integrate out high-lying particle and hole states from momentum shells around the Fermi surface as proposed by Shankar. The renormalization group approach allows for a systematic calculation of induced interactions and yields similar contributions to the scattering amplitude as the two-body parquet equations. We review results for the  $^1S_0$  and  $^3P_2$  superfluid pairing gaps as well as the spin dependence of effective interactions in neutron matter. Implications for the cooling of neutron stars are discussed.

### 1. Introduction

Conventional precision nucleon-nucleon (NN) interactions are well-constrained by two-nucleon scattering data only for laboratory energies  $E_{\text{lab}} \lesssim 350$  MeV. As a consequence, details of nuclear forces are not constrained for relative momenta  $k > 2.0 \text{ fm}^{-1}$  or for relative distances  $r < 0.5$  fm. All these NN potentials have repulsive cores, which lead to significant probing of the model-dependent high-momentum components in few and many-body applications. This model dependence, when not compensated by three-body interactions, results in the Tjon and Coester lines.

Using the renormalization group (RG), we have integrated out the high-momentum modes above a cutoff  $\Lambda$  in momentum space. The resulting low-momentum interaction, called  $V_{\text{low } k}$ , only has momentum components below the cutoff and evolves with  $\Lambda$  so that all low-energy two-body observables below the cutoff (phase shifts and deuteron binding energy) are invariant. We have shown that for  $\Lambda \lesssim 2.0 \text{ fm}^{-1}$ , all NN potentials that fit the scattering data and include the same long-distance pion physics lead to the same “universal” low-momentum interaction  $V_{\text{low } k}$ .<sup>1,2</sup> When  $V_{\text{low } k}$  is augmented by a low-momentum three-nucleon (3N) force, which regulates  $A = 3, 4$  binding energies, we find that the 3N parts are perturbative for  $\Lambda \lesssim 2.0 \text{ fm}^{-1}$ .<sup>3</sup> By perturbative we mean  $\langle \Psi^{(3)} | V_{3N} | \Psi^{(3)} \rangle \approx \langle \Psi^{(2)} | V_{3N} | \Psi^{(2)} \rangle$ , where  $|\Psi^{(n)}\rangle$  are exact solutions including up to  $n$ -body forces.

Since  $V_{\text{low } k}$  does not have a strong core at short distances, it can be used directly in many-body applications without a  $G$  matrix resummation. Fig. 1 shows the equation of state (EoS) of pure neutron matter obtained in the Hartree-Fock (HF) approximation.<sup>4</sup> In symmetric nuclear matter, saturation is due to the 3N force.<sup>5</sup>

\*Present address: Nuclear Theory Center, Indiana University, Bloomington, IN 47408.

2 Achim Schwenk

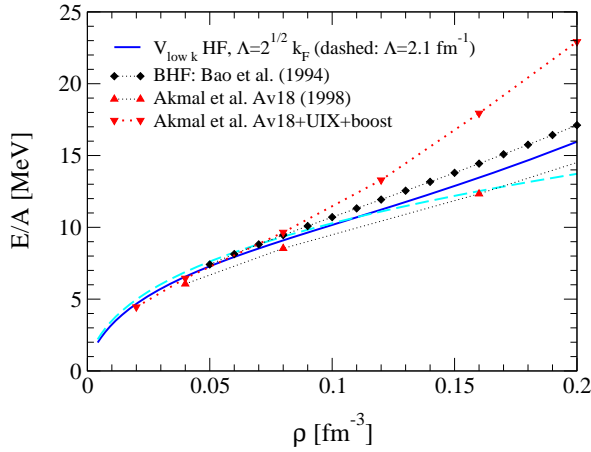


Fig. 1. Comparison of the  $V_{\text{low } k}$  HF EoS for pure neutron matter with Brueckner-Hartree-Fock (BHF) results using the Bonn potential and results of Akmal *et al.* obtained using chain summation methods, for references see.<sup>4</sup> Calculations indicate that nuclear matter may be perturbative with low-momentum interactions.<sup>5</sup> Contrary to all other microscopic interactions,  $V_{\text{low } k}$  yields bound nuclei on the HF level.<sup>6</sup>

## 2. Renormalization group approach to neutron matter

A central challenge in nuclear many-body theory lies in understanding nuclear data and predicting input for astrophysical simulations from microscopic nuclear interactions. In these proceedings, we review results for the superfluid pairing gap, where many-body correlations are crucial even in the perturbative limit, due to the singular dependence of the gap on the interaction. For dilute neutrons interacting through an attractive S-wave scattering length  $a_S < 0$  only, the pairing gap is given by<sup>7</sup>

$$\begin{aligned} \Delta &= \frac{8}{e^2} \varepsilon_F \exp \left\{ \text{const.} \left( \begin{array}{c} \text{X} \\ \text{X} \end{array} + \begin{array}{c} \text{X} \\ \text{X} \end{array} + \begin{array}{c} \text{X} \\ \text{X} \end{array} + \dots \right)^{-1} \right\} \\ &= \frac{8}{e^2} \varepsilon_F \exp \left( \frac{2}{\pi k_F a_S} + \log(0.45) + \mathcal{O}(k_F a_S) \right), \end{aligned} \quad (1)$$

where the second-order diagrams are projected on S-wave and  $e$  is the exponential constant. Thus, particle-hole (ph) polarization effects reduce the pairing gap by a factor  $(4e)^{-1/3} \approx 0.45$  compared to the mean-field BCS estimate, due to long-range spin fluctuations. In neutron matter, it is therefore crucial to include ph correlations through the induced interaction for a realistic assessment of polarization effects.

In many-body systems, the RG provides a systematic tool to construct non-perturbative effective interactions among valence nucleons. We have applied the RG to neutron matter, restricting the effective interaction to low-lying states in the vicinity of the Fermi surface.<sup>4</sup> This follows the RG approach to interacting Fermi systems proposed by Shankar.<sup>8</sup> The method is widely used in condensed matter physics to study the interference of different instabilities, especially in the context of the 2d Hubbard model.<sup>9</sup> Starting from  $V_{\text{low } k}$  in the full space, the RG generates the induced interaction, i.e., screening and vertex corrections, which contribute to the quasiparticle interaction and the low-energy scattering amplitude in the effective theory defined for particle/hole modes within a momentum shell of width  $\Lambda$

around the Fermi surface. At one loop, the change of the effective four-point vertex  $a(\mathbf{q}, \mathbf{q}'; \Lambda)$  is given by an RG equation, which reads diagrammatically

$$\frac{d}{d\Lambda} a = \text{self-energy loop} + \text{vertex correction loop} \quad (2)$$

Here, the thin lines denote intermediate states from thin momentum shells, which are integrated out successively, and the thick lines denotes “fast” particles/holes with  $|p_i - k_F| \geq \Lambda$ . The RG treats the dependence on the momenta  $\mathbf{q}$  and  $\mathbf{q}' = \mathbf{p} - \mathbf{p}'$  on an equal footing and maintains the symmetries of the scattering amplitude. Currently, we treat pairing correlations explicitly in weak-coupling BCS theory, after the RG is evolved to the Fermi surface. Future directions will include the BCS channel in the RG equation. On the Fermi surface,  $\mathbf{q}$ ,  $\mathbf{q}'$  and  $\mathbf{P} = \mathbf{p} + \mathbf{p}'$  are orthogonal, and therefore, we approximate  $a(\mathbf{q}, \mathbf{q}'; \Lambda) = a(q^2, q'^2; \Lambda)$  in the RG to extrapolate off the Fermi surface. On the  $V_{\text{low } k}$  level, the  $\mathbf{q} \cdot \mathbf{q}'$  dependence is small.

The efficacy of the RG lies in including many-body correlations from successive

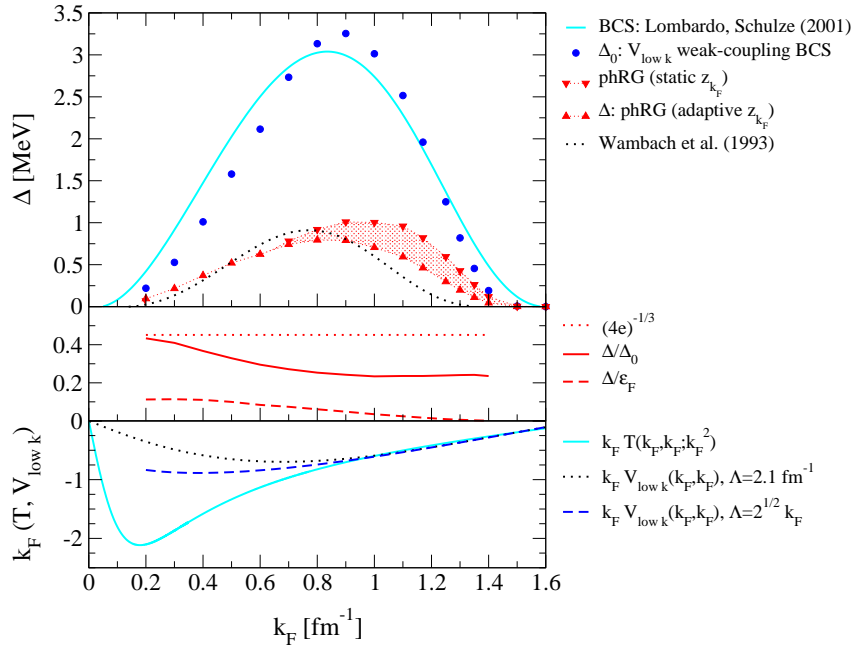


Fig. 2. Upper panel: Comparison of mean-field BCS results for the  $^1S_0$  superfluid gap to results including polarization effects through the phRG, for references and further details, including the  $z_{k_F}$  factor, see.<sup>4</sup> Middle panel: Comparison of the full superfluid gap to the mean-field BCS gap and the Fermi energy. We also show the universal extreme low-density limit,  $\Delta/\Delta_0 = (4e)^{-1/3} \approx 0.45$ . Lower panel: Comparison of dimensionless lowest-order pairing interactions.

4 Achim Schwenk

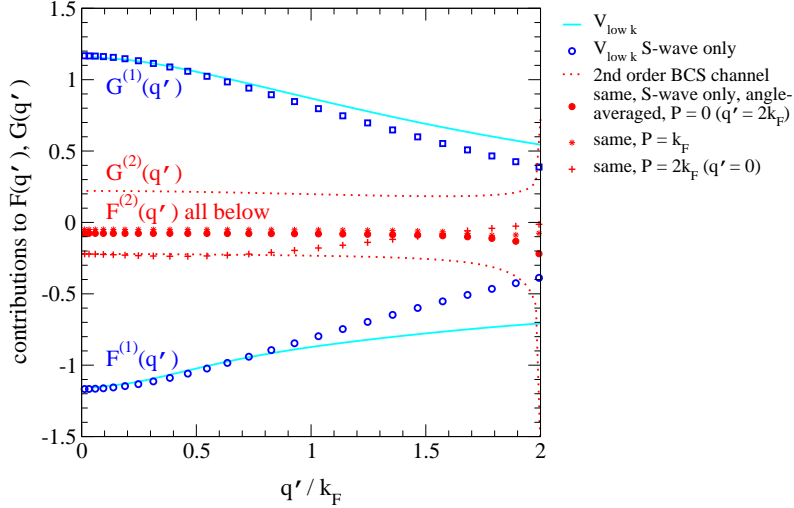


Fig. 3. Comparison of  $V_{\text{low } k}$  (1) and second-order BCS channel contributions (2) to the scalar,  $F(q')$ , and spin-spin dependent Landau functions,  $G(q')$ , in neutron matter for  $k_F = 1.0 \text{ fm}^{-1}$ . The lines are from<sup>13</sup> and the points are S-wave approximations thereof. The differences on the  $V_{\text{low } k}$  level are due to contributions from higher partial waves. Small  $q' \rightarrow 0$ , where higher partial waves are negligible in  $F^{(1)}(q')$ , correspond to  $P \rightarrow 2k_F$ . Differences for  $F^{(2)}(q')$  for larger  $q'$  are therefore due to higher partial waves, angle-averaging, as well as hole-hole contributions, which are included in the dotted lines, but not the points, and are also absent for  $P \rightarrow 2k_F$ . In contrast to free-space scattering, where the second Born term is comparable to  $V_{\text{low } k}$ , we find that the second-order particle-particle contributions are small, except for low-lying pairing correlations ( $\sim \log(P/k_F)$ ).

momentum shells, on top of an effective interaction with particle/hole polarization effects from all previous shells. By solving Eq. (2) iteratively, it can be seen that the RG builds up correlations similar to the two-body parquet equations, see also.<sup>10</sup>

In neutron matter, non-central and 3N forces are weaker, and we have solved the RG equations with the initial condition  $a(\Lambda = k_F) = V_{\text{low } k}$  including only scalar and spin-spin interactions, which dominate at low densities. In addition to the Fermi liquid parameters (see Fig. 6 in<sup>4</sup>), the RG solution yields the scattering amplitude for finite scattering angles, which is needed, e.g., for transport and pairing. In Fig. 2, we present our results for the  $^1S_0$  pairing gap. We find a suppression of the S-wave gap due to spin fluctuations from  $\Delta_0 \approx 3.3 \text{ MeV}$  to  $\Delta \approx 0.8 \text{ MeV}$  at maximum. Our results are similar to those of Wambach *et al.*,<sup>11</sup> and our mean-field ( $V_{\text{low } k}$ ) weak-coupling gap agrees well with the BCS result. This is consistent with the agreement of the  $V_{\text{low } k}$  HF EoS with the BHF results and shows that  $V_{\text{low } k}$  does not lead to strong short-range correlations. In Fig. 3, we also compare the S-wave second-order particle-particle contributions to the full second-order result.

### 3. Spin-dependence of effective interactions

Non-central forces in nuclear matter lead to novel spin-dependencies due to the presence of the Fermi sea. In addition to the standard forces, novel spin non-conserving effective interactions,  $i(\boldsymbol{\sigma}_1 - \boldsymbol{\sigma}_2) \cdot \mathbf{q} \times \mathbf{P}$  and  $(\boldsymbol{\sigma}_1 \times \boldsymbol{\sigma}_2) \cdot (\mathbf{q}' \times \mathbf{P})$ , are induced by

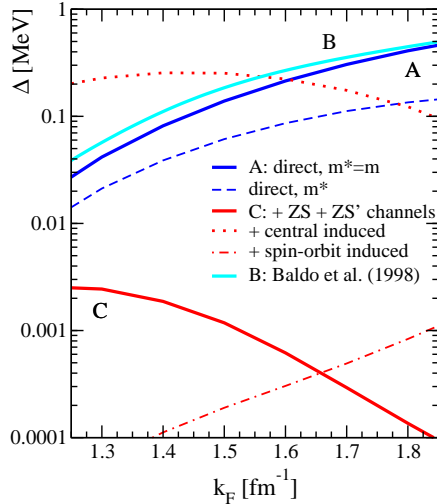


Fig. 4. The angle-averaged  ${}^3P_2$  superfluid gap versus Fermi momentum in neutron matter. The direct ( $V_{low k}$ ) weak-coupling result for a free spectrum and with effective mass is compared to the gap which includes second-order ph polarization effects on the pairing interaction. We also show the modification of the gap, if only induced central or only induced spin-orbit effects are taken into account. As a reference, we give the results of Baldo *et al.*, which are obtained by solving the BCS gap equation in the coupled  ${}^3P_2$ - ${}^3F_2$  channel for different free-space interactions. As predicted by Pethick and Ravenhall, and confirmed by our results, superfluidity is enhanced, if only central induced interactions were included. For details and references see.<sup>13</sup>

screening in the ph channels and a novel long-wavelength tensor force  $S_{12}(\mathbf{P})$  is generated.<sup>13</sup> Moreover, due to the coupling of the tensor and spin-orbit force to the strong spin-spin interaction  $G_0$ , we find that the tensor component of the quasiparticle interaction and the P-wave spin-orbit pairing force are significantly reduced in neutron matter, see Figs. 1 and 2 in.<sup>13</sup> As illustrated in Fig. 4, the screening of the spin-orbit interaction leads to a strong suppression of the  ${}^3P_2$  superfluid gap for neutrons in the interior of neutron stars. Note that in vacuum the spin-orbit force is crucial for a realistic description of the P-wave phase shifts and that the suppression of the gap is due to a reduction of the pairing interaction by only  $< 50\%$ .

Typical interior temperatures of isolated neutron star sources are on the order of  $T \sim 10^8 \text{ K} \approx 10 \text{ keV}$  and therefore it is possible to constrain the P-wave gaps phenomenologically through neutron star cooling simulations. It has been found that with free-space gaps  $\Delta_0 \sim 0.1 \text{ MeV}$ , neutron stars cool too rapidly and that a consistency with the data requires  ${}^3P_2$  gaps  $\Delta \lesssim 30 \text{ keV}$ <sup>14</sup> or  $\Delta \lesssim 10 \text{ keV}$ .<sup>15</sup> A less severe but still relevant dependence on the gap has been found in.<sup>16</sup> The same microscopic scattering amplitudes can be used to constrain neutrino emissivities.<sup>17</sup> Finally, polarization effects and novel spin-dependences are important for magnetic susceptibilities and long-wavelength spin-isospin response, as discussed in.<sup>18</sup>

Work is in progress to extend the RG approach to non-central interactions and to asymmetric matter including neutron/proton pairing.<sup>12</sup> In 2d, higher loops in the RG equation are geometrically suppressed by  $\Lambda/k_F$  for regular Fermi surfaces.<sup>8</sup> This may enable an error estimate of the one-loop truncation for low-momentum interactions, which do not scatter strongly to high-lying (high  $\Lambda$ ) states. Finally, the RG approach allows for a consistent renormalization of currents/operators and an extension to effective valence shell-model interactions for heavy nuclei.

I am grateful to Scott Bogner, Gerry Brown, Bengt Friman, Dick Furnstahl, Chuck Horowitz, Tom Kuo, Emma Olsson, Janos Polonyi and Chris Pethick for many useful discussions. This work was supported by the NSF under grant No. PHY-0098645 .

6 *Achim Schwenk*

## References

1. S.K. Bogner, T.T.S. Kuo, A. Schwenk, D.R. Entem and R. Machleidt, *Phys. Lett.* **B576**, 265 (2003), for details on the RG see nucl-th/0111042.
2. S.K. Bogner, T.T.S. Kuo and A. Schwenk, *Phys. Rep.* **386**, 1 (2003).
3. A. Nogga, S.K. Bogner and A. Schwenk, *Phys. Rev. C* (R) in press, nucl-th/0405016.
4. A. Schwenk, B. Friman and G.E. Brown, *Nucl. Phys.* **A713**, 191 (2003), for a short discussion see also nucl-th/0302081, in Hirscheegg 2003.
5. S.K. Bogner, A. Schwenk, R.J. Furnstahl and A. Nogga, in prep.
6. L. Coraggio *et al.*, *Phys. Rev.* **C68**, 034320 (2003) and nucl-th/0407003.
7. L.P. Gorkov and T.K. Melik-Barkhudarov, *Sov. Phys. JETP* **13**, 1018 (1961), see also H. Heiselberg, C.J. Pethick, H. Smith and L. Viverit, *Phys. Rev. Lett.* **85**, 2418 (2000).
8. R. Shankar, *Rev. Mod. Phys.* **66**, 129 (1994).
9. C. Honerkamp, these proceedings, cond-mat/0411267, and references therein.
10. A. Schwenk, G.E. Brown and B. Friman, *Nucl. Phys.* **A703**, 745 (2002).
11. J. Wambach, T.L. Ainsworth and D. Pines, *Nucl. Phys.* **A555**, 128 (1993).
12. A. Schwenk, B. Friman and R.J. Furnstahl, in prep.
13. A. Schwenk and B. Friman, *Phys. Rev. Lett.* **92**, 082501 (2004).
14. D.G. Yakovlev and C.J. Pethick, *Ann. Rev. Astron. Astrophys.* **42**, 169 (2004).
15. D. Blaschke, H. Grigorian and D.N. Voskresensky, *Astron. Astrophys.* **424**, 979 (2004).
16. D. Page, J.M. Lattimer, M. Prakash and A.W. Steiner, astro-ph/0403657.
17. A. Schwenk, P. Jaikumar and C. Gale, *Phys. Lett.* **B584**, 241 (2004).
18. E. Olsson and C.J. Pethick, *Phys. Rev.* **C66**, 065803 (2002), E. Olsson, P. Haensel and C.J. Pethick, *Phys. Rev.* **C70**, 025804 (2004) and private communication.